IEEE Access
Multidisciplinary | Rapid Review | Open Access Journal

Received 10 August 2022, accepted 29 August 2022, date of publication 1 September 2022, date of current version 26 September 2022.

Digital Object Identifier 10.1109/ACCESS.2022.3203713

RESEARCH ARTICLE

Optimal Coordination of Protection Devices in Distribution Networks With Distributed Energy Resources and Microgrids

CLEBERTON REIZ, (Graduate Student Member, IEEE), AND JONATAS BOAS LEITE, (Member, IEEE)
Department of Electrical Engineering, São Paulo State University, Ilha Solteira 15385, Brazil
Corresponding author: Cleberton Reiz (cleberton.reiz@unesp.br)

This work was supported in part by the Brazilian Federal Agency for Support and Evaluation of Graduate Education (CAPES) through the Scope of the Program CAPES-PrInt, under Grant 88887.310463/2018-00 and Grant 88887.569912/2020-00, and in part by the São Paulo Research Foundation (FAPESP) under Grant 2015/21972-6 and Grant 2019/07436-5.

ABSTRACT Microgrids are promising to enhance power distribution systems' efficiency, quality, sustainability, and reliability. However, microgrids operation can impose several challenges to traditional protection schemes, like changes in the power flow direction and an increase in short-circuit currents. Microgrids can include several distributed generation technologies with different behaviours during short-circuit conditions, requiring additional protection schemes and devices. In this way, the optimized coordination of reclosers and fuses in distribution networks with directional overcurrent relays, which operate as interconnection devices, might overcome many imposed protection challenges. Regarding different generation technologies, voltage-restrained overcurrent relays and frequency relays are presented as local microgrid protection for rotative and inverter-based distributed generators, respectively. The optimized coordination of these protection devices maximizes microgrid benefits and minimizes operation drawbacks by reducing interruptions impacts and energy not supplied to consumers. This work proposes, thus, a mathematical model for the optimal coordination of protection devices in distribution networks with distributed energy resources operating in grid-connected and islanded modes. The minimization technique of operating times using an elitist genetic algorithm with variable crossover and mutation processes is proposed, as well. The results show adequate coordination using passive and low-cost protection devices.

INDEX TERMS Microgrids, power distribution planning, power system protection, fuses, relays, genetic algorithms.

I. INTRODUCTION

The integration of distributed generators (DGs) in power distribution systems has grown exponentially due to the potential benefits of this technology. Examples of provided advantages include decentralization and diversification of the energy generation, reduction in the network loading, low environmental impact, and postponement of the expansion in transmission and distribution systems [1].

Renewable distributed energy resources (DERs) have been economically viable, encouraging consumers to produce energy and sell their surplus. However, DERs integration can cause significant changes in conventional distribution networks, creating new challenges for energy utilities. The main problems include the increase in short-circuit currents and the possibility of bidirectional power flow. These effects can compromise the interruption capacity of switchgear devices, cause miscoordination among protection relays, and even form non-intentional islanded subsystems, which generate risks for the maintenance crew [2].

Microgrids, feeder sections with loads and DGs, boost the distribution systems modernization due to their influence on expansion planning and operation. They increase reliability and save financial resources through new automation and

The associate editor coordinating the review of this manuscript and approving it for publication was Gab-Su Seo.

TABLE 1. Summary of main features from bibliographic review.

Ref.	DG	IBDG	Scheme	DOCR 51/50/67	Fuse	51V	81	Multiple TCCs
[4]			ICA	✓				
[5]			EGWO	✓				
[6]			HHO	✓				
[7]			GA	✓				
[8]			PSO	✓				
[9]			SA-LP	✓				
[19]			IPM	✓				
[17]	✓		SCA	✓				
[10]	✓		GA-LP, PSO-LP	✓				
[11]	✓		GA-LP	✓				
[3]	✓		NSGAII	✓	✓			
[12]	✓		SSA-LP	✓				✓
[16]	✓		PSO	✓				✓
[13]	✓	✓	GA, PSO, TLBO	✓				✓
[14]	✓	✓	GA	✓				✓
[15]	✓	✓	GA	✓				✓
PM	✓	✓	GA	✓	✓	✓	✓	✓

EGWO: Enhanced Grey Wolf Optimization; HHO: Harris Hawks Optimization; ICA: Imperialist Competitive Algorithm; IPM: Interior Point Method; LP: Linear Programming; NSGAII: Non-dominated Sorting GA II; PSO: Particle Swarm Optimization; SA: Simulated Annealing.

communication technologies. Such characteristics include microgrids in the smart grid concept, but the maximization of microgrids' benefits and minimization of possible operation difficulties must be appropriately designed and coordinated with suitable protection devices.

Directional overcurrent relays (DOCRs) are usually employed in distribution networks to allow microgrids to operate properly [3]. This equipment comprises functions ANSI 51, 50, and 67. Several research works use evolutionary algorithms to solve the optimal coordination problem of protection devices in distribution networks with DGs [3], [4], [5], [6], [7], [8], [9], [10], [11], [12], [13], [14], [15], [16], [17]. Overcurrent relays (OCRs) depend on the time dial setting (TDS) and the pickup current setting [18]. The linearization of the operating time function is a recurrent method to improve the resolution process performance [9], [10], [11], [12], despite simplifying the optimal coordination problem. Besides, some research works consider different time-current curves (TCC), expanding the possible solutions for the optimal coordination problem [12], [13], [14], [15]. Table 1 summarizes the main features in both specialized literature and the proposed methodology (PM).

Most research works in this area focus on sub-transmission systems with DOCRs [4], [5], [6], [7], [8], [9], [16], [17], [19]. A few works consider reclosers and fuses simultaneously into distribution networks with microgrid protection systems [3]. Another gap in specialized literature is about microgrids' local protection that guarantees the proper operation during short-circuit conditions within microgrids. Protection devices from distribution networks and points of common coupling (PCC) must coordinate simultaneously with microgrids' local protection. Although the practical application of frequency relays is common in inverter-based DGs (IBDGs), this technology is rarely present in literature papers on the optimal coordination problem, especially in obtaining the coordination of frequency relays with OCRs. In DGs protection schemes, most energy utilities recommend frequency relays and voltage-restrained OCRs, ANSI 81 and 51V. Therefore, 51V relays can be an attractive solution to protect rotating DGs, while frequency relays protect IBDGs to avoid miscoordination regarding their low contribution to short-circuit currents.

This work proposes, hence, a mathematical model to solve the optimal coordination problem of protection devices in distribution networks with microgrids, including renewable distributed generation and energy storage systems. It considers the minimization of operating times of reclosers and fuses present in the distribution network, as well as the microgrid protection devices. These devices comprise DOCRs present in the PCC for each microgrid and the frequency relays or voltage-restrained OCRs installed at the point of DER connection (PoC).

The coordination of protection devices is a mixed integer nonlinear combinatorial optimization problem. Most approaches in the specialized literature solve this problem using metaheuristics because such a technique generally has better computational tractability than mixed integer nonlinear programming models, which also have no guarantee of finding the optimal solution. Some works have proposed a linearization, but this strategy simplifies the problem and frequently does not include different time-current curves or intervals for the pickup current. Among the approaches using metaheuristics, particle swarm optimization (PSO) and genetic algorithms (GA) are the most common. However, the classic PSO is inadequate for problems including discrete and continuous values, requiring additional procedures to yield better performance. Thus, this work proposes a specialized GA with elitism, in addition to variable crossover and mutation processes.

In contrast to other works, this paper addresses the coordination of traditional protection devices simultaneously with the protection devices from the PCC and local protections from the PoC. The proposed technique allows the protection system coordination for distribution networks with DGs from different technologies and also considers the islanded operation of these sources with part of distribution network loads operating as a microgrid.

The main contribution of this work includes the development of a methodology for simultaneous coordination of the protection system in distribution networks with microgrids' protection through passive and low-cost protection devices. The recommendation of distribution companies is followed by adding the ANSI 81 and 51V devices into the mathematical formulation of the protection system coordination.

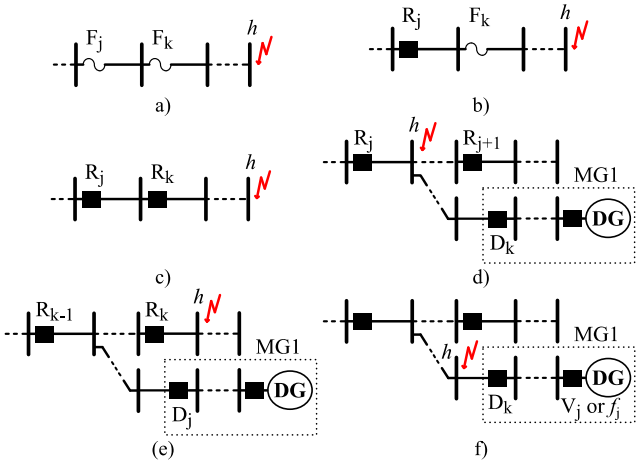

FIGURE 1. Example systems with different protection setups and fault location.

II. COORDINATION PROBLEM FORMULATION

Traditional protection schemes in distribution networks, Fig. 1 (a), (b), and (c), added with DOCRs, and local microgrids' protection devices (Fig. 1 (d), (e), and (f)) allow the integration of microgrids and, consequently, guarantee their proper operation, either in parallel or islanded modes. The DOCR must protect the PCC of microgrids by identifying external faults and by acting in both situations, which are temporary and permanent faults. Likewise, PoC protection devices are responsible for disconnecting all DERs from the microgrid during internal fault events, sending a signal to open the circuit at the PCC to minimize power outage. In this case, voltage-restrained OCRs are employed for rotating DGs, while IBDGs use frequency relays because these technologies provide less contribution for short-circuit currents than rotating DGs, [20], [21].

The operating times of OCRs are based on IEC 60255-8 [18]. Constants a and C define the curve type (1). During a fault event, the definite time characteristic, 50TD, trips first in order to maximize the continuity of energy service mitigating temporary faults. After a pre-defined sequence of reclosing shots, the 50TD characteristic is blocked. If necessary, the relay can trip again using inverse-time current curves for permanent faults. Five TCCs are considered as follows: normal inverse (NI), very inverse (VI), extremely inverse (EI), short-time inverse (SI), and long-time inverse (LI).

$$t^{51} = TMS \frac{C}{\left(\frac{I}{I_p}\right)^a - 1} \tag{1}$$

Fuses' behaviour is calculated using linear interpolation with samples provided by the manufacturer [22].

IIDs are also based on (1) for permanent faults and 50TD for temporary ones. Moreover, these devices include a directional unit to allow their operation in only one direction, that is, for faults external to the microgrid.

The operating times of 51V relays are also based on (1), but the pick-up current is previously multiplied by the voltage on the PoC in pu, as in (2).

$$t^{51V} = TMS \frac{C}{\left(\frac{I}{V^{51V} I_p}\right)^a - 1} \tag{2}$$

TABLE 2. Frequency relay response.

Frequency intervals (Hz)	Clearing time
$\Delta f \geq 3.5$	Instantaneous
$2.5 < \Delta f < 3.5$	5s
$1.5 < \Delta f < 2.5$	10s
$\Delta f \leq 1.5$	Shall not trip

Frequency relays from microgrids' PoCs with IBDGs consider the frequency limits defined by IEEE 1547 [23]. The frequency estimation is based on the DG power change between normal and short-circuit conditions and the system's inertia. During a short-circuit event, the power demand suddenly increases, leading to an increment in the mechanic power due to the machines' control response. Since DGs controller tends to reduce the difference between primary and electric power, the greatest unbalance occurs at the beginning of the short-circuit event, i.e., the difference between pre- and post-fault generated power. In (3), ΔP is the power unbalance, H_{sys} is the system's inertia, and Δf is the frequency deviation in the time domain, [24], [25]. The frequency deviation rate performs a similar behaviour, starting with the highest value and decreasing over time.

$$\Delta P = 2H_{Sys} \frac{d\Delta f}{dt} \tag{3}$$

Among DERs, wind turbines have a significant amount of kinetic energy in their blades, which is essential to consider in the system's inertia estimation in addition to conventional machines [25]. Biomass generators can be represented as dispatchable DG, being considered a conventional machine. PV units have almost no contribution to the system's inertia. The sum of total inertia constants due to conventional and wind turbines, H_C and H_W, respectively, is shown in (4), where Nc and Nw are the amounts of each turbine.

$$H_{sys} = H_C + H_W = \sum_{i=1}^{Nc} H_{Ci} + \sum_{i=1}^{Nw} H_{Wi} \tag{4}$$

Thus, the aforementioned features allow the frequency estimation and, consequently, the necessary information for coordinating frequency relays with microgrids' IIDs. Operating times of ANSI 81 relays are time defined and depend on the frequency deviation level, presenting four conditions, as described in Table 2.

The proposed protection and control scheme can also be extended to the coordination and selectivity of protection devices inside microgrids during the islanded operation mode. However, this work focuses on the grid-connected mode assuming the entire distribution network topology. The protection system properly operates for any fault events in such conditions.

A. PROTECTION DEVICES PARAMETRIZATION

Several nominal current values are employed for protection devices parameterization [3]. Fig. 1 (a) shows an example system with two fuses. The upstream protection device is defined as the protected device represented by j, while the closest one to fault is the protective device, represented by k. Also, the index u is considered in some cases of this section, representing an upstream protected device concerning j and k.

The coordination between fuses is ensured using (5), where the total-clearing (TC) fuse time, t_{Fk}^{TC}, is less than or equal to k_{coord}^{MM-TC} times the minimum-melting (MM) fuse time, t_{Fj}^{MM}, which depend upon minimum single-phase fault current with a resistance of 40 Ω, $I_{40}^{1\emptyset}$.

$$k_{coord}^{MM-TC} t_{Fj}^{MM}\left(I_{40_{Fj-h}}^{1\emptyset}\right) \geq t_{F_k}^{TC}\left(I_{40_{Fk-h}}^{1\emptyset}\right) \tag{5}$$

The minimum pickup current of reclosers is set at different intervals for phase and neutral units [3]. Coordination and selectivity of fuses with reclosers are accomplished using three distinct faults to ensure the sensitivity within a well-defined interval for different protection system functions. In coordination, $I_{40}^{1\emptyset}$ determines the lower limit of the sensitivity region, while a fault with 20 Ω of impedance, $I_{20}^{1\emptyset}$, establishes the upper limit. Neutral units use the zero sequence short-circuit current, indicated in each fault by z. The selectivity takes into account $I_{40}^{1\emptyset}$ and the solid single-phase fault, $I_0^{1\emptyset}$. The fault current $I_0^{1\emptyset}$ is only used in the selectivity between reclosers and fuses because of higher short-circuit currents in feeder sections closer to the substation. This characteristic melts the fuse faster than the minimum recloser's operating time in the 50TD function for most available fuses, making coordination impossible.

In Fig. 1 (b), the coordination and selectivity between OCR and fuse are guaranteed by (6) and (7) for functions 50 and 51, respectively. Note that the protected device in (6) is the fuse, while in (7), it is the primary protection. Thus, the subscripts j and k exchange their positions in (6) concerning Fig. 1 (b).

The coordination factor of characteristic 50, k_{coord}^{MM-50}, depends on the number of reclosing operations. The coordination time, t_{coord}^{51-TC}, ensures a safety margin between devices operating time [3]. Superscript index, like $MM-50$, indicates firstly the slower protective device or function from the pair.

$$t_{Fj}^{MM}\left(I_{40_{Fj-h}}^{1\emptyset}\right) \geq k_{coord}^{MM-50} t_{Rk}^{50}\left(I_{40_{Rk-h}}^{1\emptyset}\right) \tag{6}$$

$$t_{Rj}^{51}\left(I_{40_{Rj-h}}^{1\emptyset}\right) \geq t_{Fk}^{TC}\left(I_{40_{Fk-h}}^{1\emptyset}\right) + t_{coord}^{51-TC} \tag{7}$$

The coordination sensibility between distribution network reclosers is ensured using faults $I^{2\emptyset}$ and $I_{40}^{1\emptyset}$ for the phase units and $I_{0z}^{1\emptyset}$ and $I_{40z}^{1\emptyset}$ for neutral units. In Fig. 1 (c), there is an example system with two reclosers, Rj and Rk. Coordination and selectivity are achieved through (8) and (9), where t_{coord}^{50-50} and t_{coord}^{51-51} are coordination times, respectively.

$$t_{Rj}^{50}\left(I_{Rj-h}^{2\emptyset}\right) \geq t_{Rk}^{50}\left(I_{Rk-h}^{2\emptyset}\right) + t_{coord}^{50-50} \tag{8}$$

$$t_{Rj}^{51}\left(I_{Rj-h}^{2\emptyset}\right) \geq t_{Rk}^{51}\left(I_{Rk-h}^{2\emptyset}\right) + t_{coord}^{51-51} \tag{9}$$

DOCRs have a smaller interval for pickup currents than distribution network reclosers because lower magnitude currents flow through the PCC branch, depending on the microgrid capacity. At the same time, the upper limit must be small since IBDGs also have a small short-circuit current contribution during a fault condition [21].

Coordination and selectivity between DOCRs and reclosers consider fault currents $I^{2\emptyset}$ and single-phase fault currents with 5 Ω impedance, $I_5^{1\emptyset}$, for phase units. Neutral units use the zero sequence short-circuit currents $I_{0z}^{1\emptyset}$ and $I_{5z}^{1\emptyset}$. Users can set longer ranges, but the ride-through requirements must be taken into account. The same faults are considered for selectivity between 51V relays and DOCRs.

Fig. 1 (d) shows an example system with a microgrid, MG1, between reclosers Rj and $Rj+1$. For a fault in Rj protected feeder section, we assume that Dk must trip faster than Rj for permanent (10) and temporary faults (11). In Fig. 1 (e), the example system is a microgrid with a fault in the protection zone of the downstream recloser Rk. During permanent or temporary faults in Rk protected section, Dj must trip slower than Rk, avoiding unnecessary MG1 disconnection, as respectively given in (12) and (13). Coordination times t_{coord}^{51-D}, t_{coord}^{D-51}, t_{coord}^{50-D}, and t_{coord}^{D-50} ensure the coordination and selectivity between such devices.

$$t_{Rj}^{51}(I_{Rj-h}^{2\emptyset}) \geq t_{Dk}^{51}(I_{Dk-h}^{2\emptyset}) + t_{coord}^{51-D} \tag{10}$$

$$t_{Rj}^{50}(I_{Rj-h}^{2\emptyset}) \geq t_{Dk}^{50}(I_{Dk-h}^{2\emptyset}) + t_{coord}^{50-D} \tag{11}$$

$$t_{Dj}^{51}(I_{Dj-h}^{2\emptyset}) \geq t_{Rk}^{51}(I_{Rk-h}^{2\emptyset}) + t_{coord}^{D-51} \tag{12}$$

$$t_{Dj}^{50}(I_{Dj-h}^{2\emptyset}) \geq t_{Rk}^{50}(I_{Rk-h}^{2\emptyset}) + t_{coord}^{D-50} \tag{13}$$

Fig. 1 (f) shows a microgrid with a fault near the PCC. The selectivity between 51V relay and IID is ensured using (14) for a fault outside the microgrid, where t_{coord}^{V-D} is the coordination time. The index V represents 51V relays acting as local protection in microgrids' PoC.

$$t_{Vj}^{51}(I_{Vj-h}^{2\emptyset}) \geq t_{Dk}^{51}(I_{Dk-h}^{2\emptyset}) + t_{coord}^{V-D} \tag{14}$$

Frequency relays must trip if the frequency drift surpasses some intervals established by IEEE 1547, as presented in Table 2. Each frequency interval has a clearing time limit, depending on the variation level. For a fault outside the microgrid, as shown in Fig. 1 (f), the IID should trip first than the frequency relay (15). Some particular cases require the instantaneous operation of the frequency relay, making coordination impossible. The proposed method does not perform the coordination in such cases.

$$t_{fj}^{81}\left(I_{fj-h}^{2\emptyset}\right) \geq t_{Dk}^{51}\left(I_{Dk-k}^{2\emptyset}\right) + t_{coord}^{f-D} \tag{15}$$

B. OBJECTIVE FUNCTION AND CONSTRAINTS

The proposed penalized objective function (POF) in (16) is based on [26], for reducing the operating times of protection devices, which is the goal objective, in addition to penalties if some constraint is exceeded. The first equation block includes

all operating times, previously multiplied by an α factor to weight the relevance of this part. Factors β and γ have the role of weighting penalties.

From left to right, the first sum refers to the operating times of reclosers (R), DOCRs (D), and 51V (V) relays (set represented by $\boldsymbol{r}$), where N_r is the amount of each protective device, $N_r = N_R + N_D + N_V$. The second sum refers to the operating times of fuses (F), where N_F is the number of this device. The third and fourth sums refer to penalties whenever the selectivity and coordination constraints are exceeded. The first includes the set $\boldsymbol{\varphi}$ related to selectivity between fuses or pairs with 51 OCR function. The fifth sum includes the set $\boldsymbol{\varepsilon}$ that is related to characteristic 50. Functions 50 and 51 have significant operating time differences, so it is important to weigh them separately. Parameters N_φ and N_ε contain the total quantity of each pair of protection devices.

$$\begin{aligned} POF = \min \Bigg[& \alpha \left(\sum_{i=1}^{N_r} t_{ri} + \sum_{i=1}^{N_F} t_{Fi} \right) \\ & + \beta \sum_{i=1}^{N_\varphi} \left(\left| \Delta t_i^{\varphi} - \left| \Delta t_i^{\varphi} \right| \right| \right) \\ & + \gamma \sum_{i=1}^{N_\varepsilon} \left(\left| \Delta t_i^{\varepsilon} - \left| \Delta t_i^{\varepsilon} \right| \right| \right) \Bigg] \end{aligned} \tag{16}$$

Equations (17)-(22) represent the penalties for the set of pairs $\boldsymbol{\varphi}$, while (23)-(26) are employed for the set of pairs $\boldsymbol{\varepsilon}$. In that order, protected and protective devices are always represented by j and k.

$$\Delta t_i^{51} = t_{Rj}^{51} - t_{Rk}^{51} - t_{coord}^{51-51} \tag{17}$$
$$\Delta t_i^{51-F} = t_{Rj}^{51} - t_{Fk}^{TC} - t_{coord}^{51-TC} \tag{18}$$
$$\Delta t_i^{F} = k_{coord}^{MM-TC} t_{Fj}^{MM} - t_{Fk}^{TC} \tag{19}$$
$$\Delta t_i^{D-51} = t_{Dj}^{51} - t_{Rk}^{51} - t_{coord}^{D-51} \tag{20}$$
$$\Delta t_i^{V-D} = t_{Vj}^{51} - t_{Dk}^{51} - t_{coord}^{V-D} \tag{21}$$
$$\Delta t_i^{f-D} = t_{fj}^{81} - t_{Dk}^{51} - t_{coord}^{f-D} \tag{22}$$
$$\Delta t_i^{50} = t_{Rj}^{50} - t_{Rk}^{50} - t_{coord}^{50-50} \tag{23}$$
$$\Delta t_i^{F-50} = t_{Fj}^{MM} - k_{coord}^{MM-50} t_{Rk}^{50} \tag{24}$$
$$\Delta t_i^{D-50} = t_{Dj}^{50} - t_{Rk}^{50} - t_{coord}^{D-50} \tag{25}$$
$$\Delta t_i^{50-D} = t_{Rj}^{50} - t_{Dk}^{50} - t_{coord}^{50-D} \tag{26}$$

C. GENETIC ALGORITHM

The solution technique for the optimal coordination problem uses a dedicated GA due to its simplicity and easiness in solving nonlinear combinatorial optimization problems with low processing time [27]. A set of solutions represents the population, and those solutions are composed by a set of elements, representing the genes of each individual. Fig. 2 shows an example of the solution coding used in the proposed GA. Thus, the strongest individuals (encoded solutions) survive during the optimization process by transmitting to their descendants the best genes through genetic operators such as selection, crossover, and mutation. The selection stage randomly chooses two pairs of individuals from a population and compares their quality (POF value). The best individual from each pair goes through the crossover process.

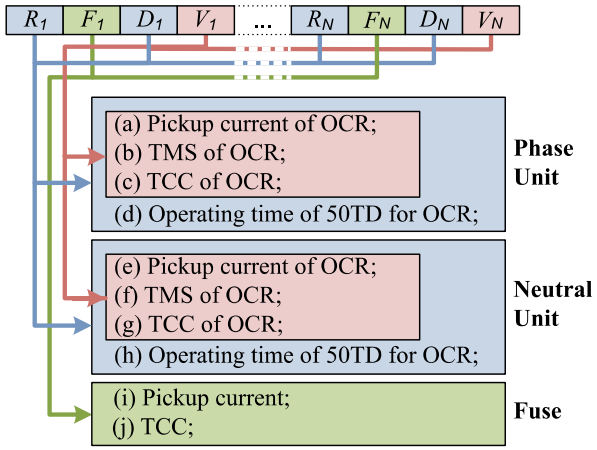

FIGURE 2. GA coding employed in the proposed methodology.

In the crossover stage, genetic material is exchanged between selected individuals. Genes are randomly mixed, creating a new pair of individuals that will compose the new population. The crossover process is variable, randomly modifying the individual genes [28]. The crossover rate, ρ_c, can vary according to (27). Such an approach prevents exploration restricted only to local solutions. The number of similar solutions is represented by SI_i in the i-th generation, i.e., similar solutions concerning other population individuals, η_p. The adjustment factor k_{min}^c defines a minimum crossover rate to the GA process, while k_{max}^c is the maximum. Thus, the crossover process starts at high rates and decreases as the population loses its diversity. Before including the crossover individuals in the new population, the mutation process begins.

$$\rho_c = k_{max}^c - \frac{SI_i}{\eta_p}(k_{max}^c - k_{min}^c) \tag{27}$$

The population mutation rate, ρ_m, can also vary according to the same concept, as is given in (27). Unlike the crossover process, the mutation rate increases as similar individuals in the population increase. In this case, the factors k_{min}^m and k_{max}^m exchange their positions and the superscript m is employed, representing the mutation parameters (28).

$$\rho_m = k_{max}^m - \frac{SI_i}{\eta_p}(k_{max}^m - k_{min}^m) \tag{28}$$

The elitism technique allows a more efficient exchange of genetic material between population individuals and is frequently applied in the specialized literature [28]. Therefore, such a technique is also applied in the proposed methodology.

Fig. 2 shows, from (a) to (j), the genes considered on each chromosome as a row of numeric values that represent adjustment parameters of protection devices. Constraints of protection devices' parameters involve: (29)-(33) for reclosers and DOCRs; (34)-(35) for fuses; and (29)-(31) and (33) for local protection of rotating DGs. Maximum and minimum values

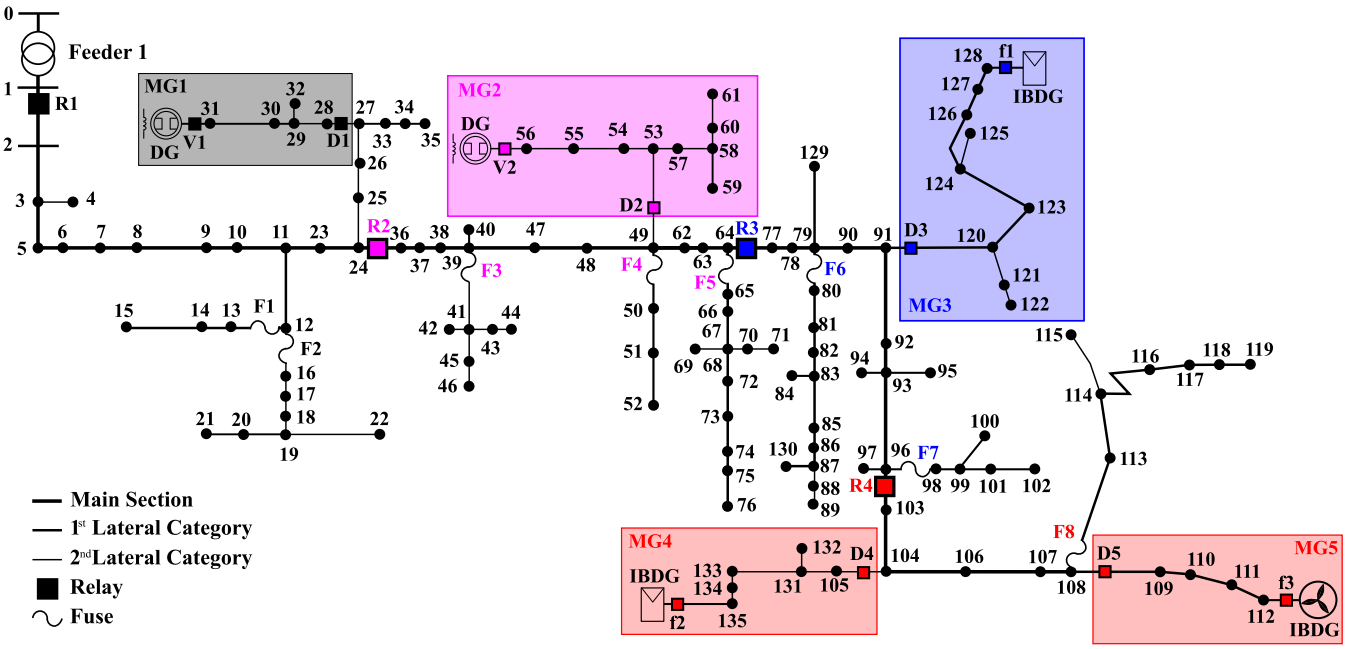

FIGURE 3. Distribution test system.

for constants k_{51P}, TMS, TCC, t^{50TD}, k_{51N}, I_F^{nom}, and $Type^F$ are indicated by over and under bars, respectively.

$$\underline{k_{51P}} I_{load_i}^{max} \leq Ip_i^{51P} \leq \overline{k}_{51P} I_{load_i}^{max} \tag{29}$$

$$\underline{\text{TMS}} \leq TMS_i \leq \overline{TMS} \tag{30}$$

$$\underline{TCC} \leq TCC_i \leq \overline{TCC} \tag{31}$$

$$\underline{\text{t}^{50\text{TD}}} \leq \text{t}_i^{50\text{TD}} \leq \bar{\text{t}}^{50\text{TD}} \tag{32}$$

$$\underline{k_{51N}} I_{load_i}^{max} \leq Ip_i^{51N} \leq \overline{k}_{51N} I_{load_i}^{max} \tag{33}$$

$$\underline{I_F^{nom}} \leq I_{F_i}^{nom} \leq \overline{I}_F^{nom} \tag{34}$$

$$\underline{Type^F} \leq Type_i^F \leq \overline{Type}^F \tag{35}$$

D. SHORT-CIRCUIT ESTIMATION

Power flow results during a short-circuit event are estimated using Thevenin's equivalent circuit and the three-phase bus impedance matrix.

The short-circuit current is calculated by multiplying the inverse of the equivalent impedance at the faulted bus f by the pre-fault voltage at the same bus. Such current values allow updating the post-fault voltage profiles replacing (36) into (37), where ΔV_i is the voltage variation, Z_{if}^B and Z_{iG}^B are off-diagonal elements of the bus impedance matrix concerning fault and DG buses, respectively. $V_i(0)$ and $V_i(F)$ are the pre- and post-fault voltage.

The short-circuit current J_{fI} also includes the contribution of rotating DGs, which are represented as voltage sources. Thus, their contribution to the short-circuit is included by performing the Kron reduction for each line with DGs' impedance. On the other hand, IBDGs' contribution, J_{fII}, is considered in the post-fault voltage using (38), where Z_{ff}^B is the diagonal element of the bus impedance matrix, Z_{fm}^B is an off-diagonal element of the DG m, and J_m is the pre-fault current of the same DG, multiplied by a factor λ.

$$\Delta V_i = Z_{if}^B J_{fI} + Z_{iG}^B J_{fII} \tag{36}$$

$$V_i(F) = V_i(0) + \Delta V_i \tag{37}$$

$$J_{fII} = \frac{1}{Z_{ff}^B} \sum_{m=1}^{n} Z_{fm}^B J_m(0)\lambda \tag{38}$$

III. TESTS AND RESULTS

Fig. 3 shows a 135-bus unbalanced distribution system employed to evaluate the proposed methodology. This network has 13.8kV and 7.065 MVA [29]. The protection system without microgrids consists of four reclosers and eight fuses. Five microgrids (MG) are then installed in the 135-bus system, where MG1 and MG2 are supplied by rotating DGs. MG3 and MG4 are supplied by photovoltaic panels with energy storage systems, while a full-converter wind DG supplies MG5 also with energy storage. Microgrids have the same nominal capacity, and their total power represents 30% of the total system's load demand, with a power factor of 0.92.

The proposed method is implemented in C++ general programming language due to its speed and computational efficiency. Tests were performed on a personal computer with Intel(R) Core(TM) i7-7700, 3.60 GHz, and 16GB of RAM.

A. PROTECTION DEVICES PARAMETRIZATION

GA resolution depends on the previous adjustment of factors α (alpha), β (beta), and γ (gamma), where the first one emphasises the objective function (OF) while the others are dedicated to the penalties. Thus, these factors must be greater than α to avoid finding unfeasible solutions.

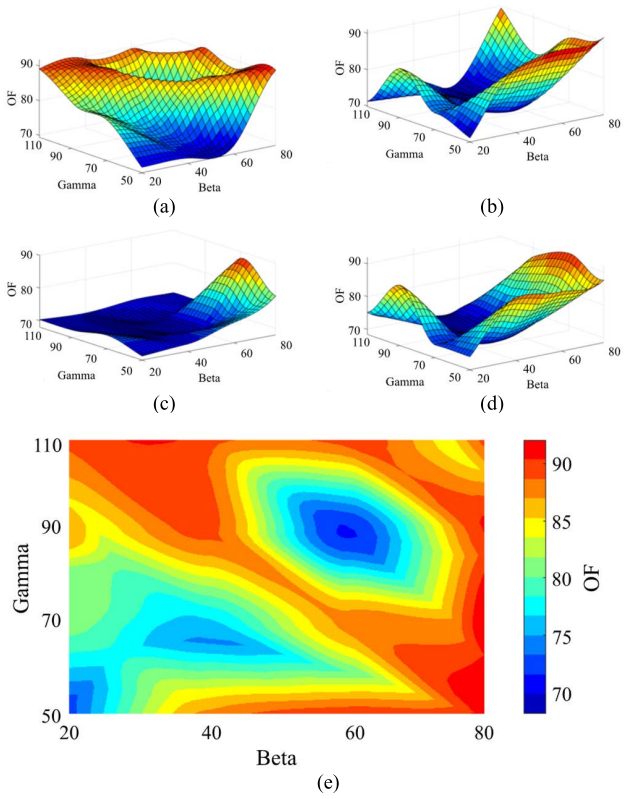

FIGURE 4. OF results using different factors' values.

Several tests were performed to achieve the most suitable value for each factor. The interval for β and γ was defined as 0-200, and 1-4 for α. However, depending on the values adopted for these weighting factors, the GA may not find feasible solutions due to the weight assigned to the penalties. For β and γ as 0-20 and 0-50, respectively, the results are not constant or asymptotic, and part of them are infeasible. On the other hand, for intervals of β and γ as 80-200 and 110-200, respectively, solutions are feasible, but the objective function is higher than using intervals shown in Fig. 4. Thus, for β and γ, the intervals shown in Fig. 4 are 20-80 and 50-110, respectively. Fig. 4 (a), (b), (c), and (d) consider α equal to 1, 2, 3, and 4, in that order. Fig. 4 (e) overlaps the previous figures with OF values identified by the temperature map. All tests consider a population of 1500 and 500 generations.

Results from Fig. 4 (a), (b), (c), and (d) show that the OF has worse values when β is close to or high than γ. In fact, the penalties of instantaneous operating times are multiplied by γ, and such penalty times are generally small compared with those related to fuses and time overcurrent relays, which are multiplied by β. Thus, instantaneous operating times can have more difficulties in reaching feasibility using these factors. Therefore, better results are achieved when higher γ values are considered concerning β.

Fig. 4 (c) presents better OF results using $\alpha = 3$ compared to other cases. Almost all intervals considered for β and γ provide good results, excluding the aforementioned cases

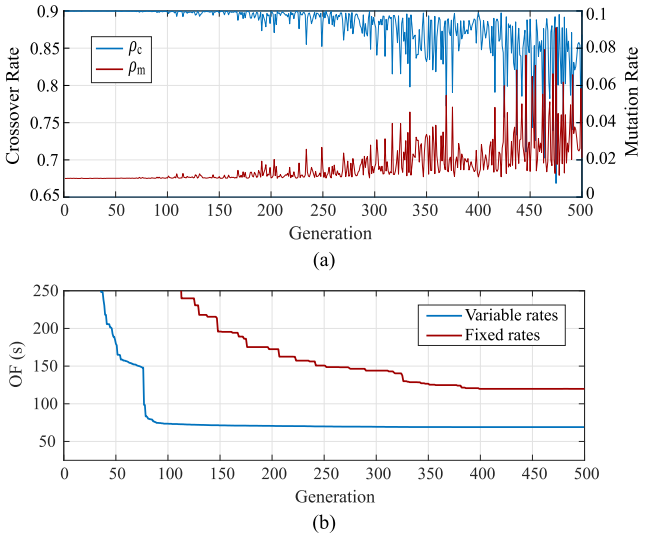

FIGURE 5. GA behaviour during the resolution process: a) Crossover and mutation behaviour using variable rates; and b) OF behaviour using fixed and variable mutation and crossover rates.

when β is equal to or higher than γ. Fig. 4 (e) shows that using β and γ equal to 60 and 90 provides good results for all values of α. Therefore, the most suitable values are 3, 60, and 90 for factors α, β, and γ, respectively. The best OF result in the sensibility analysis was achieved using these values. Similar tests were performed for tunning variable crossover and mutation rates, generation number, and population size.

The number of generations and the population size are equal to 500 and 1500, respectively, while maximum and minimum crossover and mutation rates are 0.9, 0.5, 0.15, and 0.01. Elite solutions represent 1% of the current population. Such settings are updated every generation.

A graph of crossover and mutation is shown in Fig. 5 (a). Rates show a mirrored behaviour since the same expression is used in both variables, changing only the maximum and minimum values. The crossover rate initially has the same value as $k^c_{\max}$. The first 150 generations refine several local solutions in the search space, reducing the crossover rate slightly. Thereafter, the value changes more often because the method tries to increase population diversity whenever their similarity increases. In parallel, the mutation rate starts at k^m_{min} and increases, varying in the same proportion as the crossover rate.

The proposed model is evaluated by performing a second test with fixed rates of 0.7 and 0.075 for crossover and mutation. Fig. 5 (b) compares the OF progression in both cases, variable and fixed rates. Before 100 generations, the case using variable rates presents OF value lower than 100s, while the case using fixed rates has OF value higher than 250s. The sum of operating times for the coordination problem is 69.03s, whereas with fixed rates, the sum of operating times is 119.84s. OF results show the feasibility of the proposed methodology using variable crossover and mutation rates.

TABLE 3. Parameters considered in the coordination problem.

Parameter	Value	Parameter	Value	Parameter	Value
t_{coord}^{51-51}	0.30s	k_{coord}^{MM-50}	1.35	$\underline{t^{50TD}}$	0.02s
t_{coord}^{50-50}	0.02s	k_{coord}^{MM-TC}	0.75	$\overline{t^{50TD}}$	1.00s
t_{coord}^{51-TC}	0.30s	$\underline{k_{51P}}$	1.20	$\underline{k_{51N}}$	0.10
t_{coord}^{50-D}	0.02s	$\overline{k_{51P}}$	1.30, 1.50	$\overline{k_{51N}}$	0.30
t_{coord}^{V-D}	0.10s	$\underline{TMS}$	0.10	$\underline{I_F^{nom}}$	1
t_{coord}^{51-D}	0.10s	$\overline{TMS}$	2.00	$\overline{I_F^{nom}}$	8
t_{coord}^{D-51}	0.10s	$\underline{TCC}$	1	$\underline{Type^F}$	1 (K)
t_{coord}^{D-50}	0.02s	$\overline{TCC}$	3	$\overline{Type^F}$	2 (T)

TABLE 4. Summary of main parameters of reclosers.

Relay	I_p (A)	*TMS*	*TCC*	Protected device	Δt^{51}	t^{50TD}
R1 (P)	227.14	0.388	NI	R2, F1 e F2	0.007	0.160
R2 (P)	147.19	0.330	NI	R3, F3, F4 e F5	0.010	0.120
R3 (P)	76.48	0.257	NI	R4, F6 e F7	0.001	0.080
R4 (P)	15.61	0.973	SI	F8	-	0.040
R1 (N)	32.16	0.473	LI	R2, F1 e F2	0.000	0.161
R2 (N)	28.54	0.389	LI	R3, F3, F4 e F5	0.002	0.120
R3 (N)	9.87	0.718	LI	R4, F6 e F7	0.000	0.080
R4 (N)	3.24	0.789	LI	F8	-	0.040

B. PROTECTION DEVICES COORDINATION

Coordination intervals and other parameters for the coordination problem are shown in Table 3 [3]. For reclosers' phase units, the upper limit $\overline{k_{51P}}$ is set to 1.5, while for other relays, such a limit is set to 1.3. Operating times of ANSI 81 relays are time defined and depend on the frequency deviation level, presenting four conditions, as described in Table 2. Such conditions allow a faster relay trip than IEEE 1547 standard [23]. For 51V relays, if the voltage is outside the range between 0.25 and 1 pu the voltage in the multiplication is fixed at the nearest upper or lower limit.

The main parameters of distribution network reclosers are shown in Table 4. LI and NI TCCs are a preferred choice for distribution network reclosers because two faults are considered in the model, getting lower operating times for both points in these TCCs. Operating times in 50TD characteristic for R4 are near the minimum limit imposed by (32). However, these operating times cannot be the minimum value since R4 needs to be coordinated with DOCRs D4 and D5 of MG4 and MG5, respectively, not exceeding the coordination time t_{coord}^{50-D}.

Table 5 shows the main parameters of fuses. Type 40K is the preferred choice, except for F7 and F8, which are of type 25K because these sections have minor short-circuit currents. Fuses of type 25T are also a feasible solution for fuses F1 to F4, despite increasing operating times. The behaviour of

TABLE 5. Summary of main parameters of fuses.

Fuse	I_F^{nom}	$Type^F$	Δt^{51-F}(P)	Δt^{51-F}(N)	Δt^{F-50}(P)	Δt^{F-50}(N)
F1	40	K	0.928	0.699	0.888	0.066
F2	40	K	0.937	0.717	0.695	0.042
F3	40	K	0.596	0.409	0.845	0.105
F4	40	K	0.615	0.453	0.872	0.111
F5	40	K	0.630	0.489	0.716	0.095
F6	40	K	0.309	0.214	0.773	0.151
F7	25	K	0.322	0.239	0.285	0.006
F8	25	K	0.025	0.000	0.374	0.077

TABLE 6. Summary of main parameters of DOCRs.

Relay	I_p (A)	*TMS*	*TCC*	Pair	Δt^{50-D}	Δt^{D-51}	t^{50TD}
D1 (P)	3.272	0.143	LI	R1-D1	0.0000	0.0098	0.1404
D2 (P)	3.896	0.698	VI	R2-D2	0.0000	0.0034	0.1002
D3 (P)	8.773	0.074	SI	R3-D3	0.0001	0.0080	0.0602
D4 (P)	2.675	0.051	SI	R4-D4	0.0001	-	0.0200
D5 (P)	5.982	0.054	SI	R4-D5	0.0001	-	0.0200
D1 (N)	0.855	0.972	NI	R1-D1	0.0000	0.5199	0.1404
D2 (N)	0.731	0.868	LI	R2-D2	0.0000	0.0031	0.1003
D3 (N)	1.043	0.279	SI	R3-D3	0.0001	0.0021	0.0603
D4 (N)	0.315	0.055	SI	R4-D4	0.0001	-	0.0201
D5 (N)	0.692	0.063	SI	R4-D5	0.0001	-	0.0200

TABLE 7. Summary of main parameters 51V relays.

Relay	I_p (A)	*TMS*	*TCC*	Pair	Δt^{V-D}
V1 (P)	19.641	0.550	VI	D1-V1	0.003
V2 (P)	19.728	0.644	EI	D2-V2	0.019
V1 (N)	4.824	0.993	NI	D1-V1	0.009
V2 (N)	3.658	0.853	LI	D2-V2	0.006

fuses 25T and 40K are very similar. However, fuses 40K have slightly shorter operating times, leading the GA-based solver to choose 40K fuses.

Table 6 shows the main parameters of DOCRs. Operating times of DOCRs D4 and D5 in 50TD have the minimum value allowed by (32), except for D4 neutral unit. Hence, it is not optimal since the OF can still be improved. Nevertheless, it is a solution of excellent quality because most DOCRs units have the best time allowed by constraints. Moreover, the unit with the longest time has only a difference of 0.0001s concerning the optimal setup. Other PCC relays have higher times, mainly due to coordination restrictions with downstream reclosers.

Table 7 shows the main coordination features of 51V local protections. Coordination times of 51V relays are near the limits imposed by constraint (21), indicating the high quality of the obtained solution. Since the solution does not exceed the model's restrictions, the parameters presented provide selectivity with the distribution network protections, tripping only in case of faults internal to the microgrid.

Fig. 6 shows the coordination and selectivity between D1 with relays R1(50) and R2(50/51). Magenta dashed areas

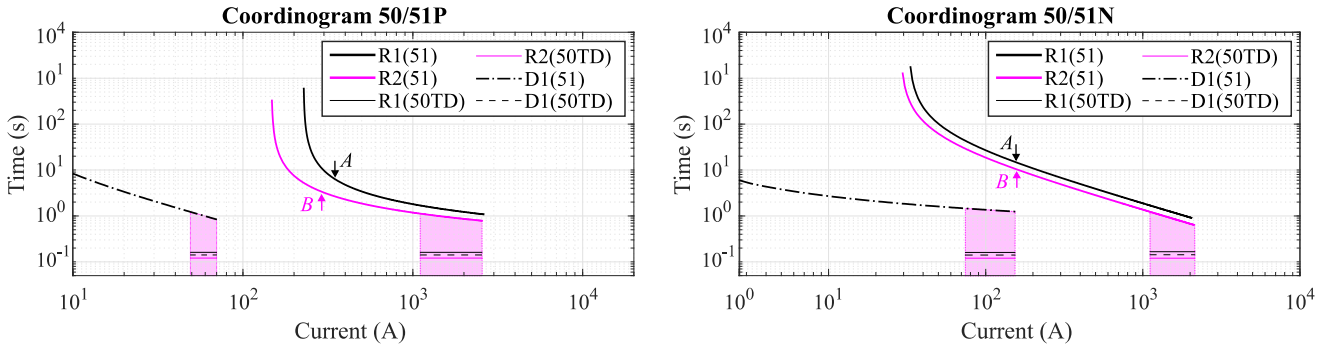

FIGURE 6. Coordination and selectivity of D1 with R1(50) and R2(50/51).

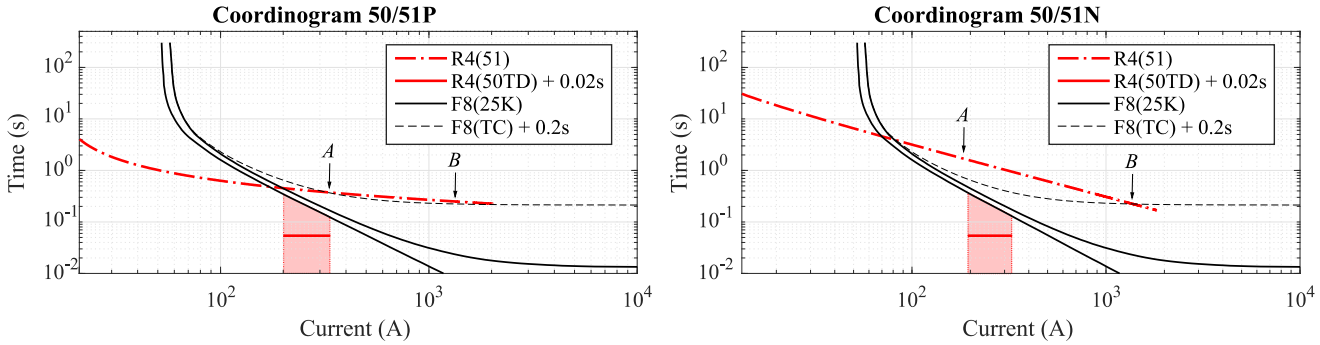

FIGURE 7. Coordination and selectivity of R4 with F8.

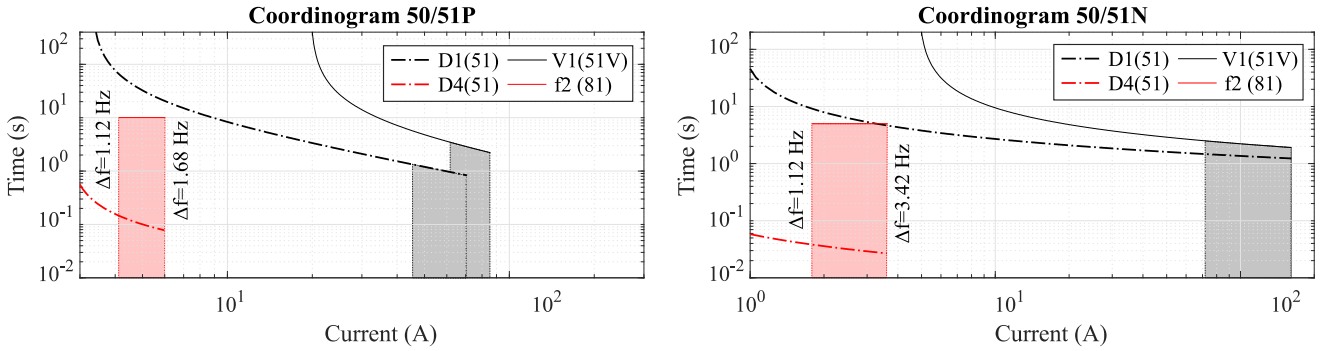

FIGURE 8. Coordination and selectivity of pairs D1-V1 and D4-f2.

show the coordination range between D1 and R2 with limits defined by $I^{2\emptyset}$ and $I_5^{1\emptyset}$ for phase units, while neutral units consider $I_{0z}^{1\emptyset}$ and $I_{5z}^{1\emptyset}$, in that order. During a short-circuit event in R2 protective area, R2 trips first than other devices in temporary and permanent faults. For a temporary fault in R1 protective area, D1 trips first than R1 to allow a safe 50TD operation. Coordination and selectivity between R1 and R2 are also shown in Fig. 6. Currents measured by reclosers R1 and R2 in the minimum range are highlighted with *A* and *B*, respectively.

Fig. 7 shows the coordination and selectivity between relay R4 with fuse F8. The black dashed line represents the TC fuse curve plus 0.2s of coordination time to ensure a proper operation. The red dashed area shows the coordination range between R1 and F8 in 50TD characteristic. The coordination range of characteristic 51 is wider, with a minimum limit defined by a single-phase fault with impedances of 40 Ω and 0 Ω for phase and neutral units, respectively. *A* and *B* highlight the minimum and maximum current values measured by the recloser for the same coordination range, in that order.

Fig. 8 shows the selectivity between D1 and V1 and between D4 and f2. For selectivity between D1 and V1, although the curves in the phase unit seem distant, the multiplication of the DG voltage in the pickup current makes the trip time between them very close, as shown in the coordination times of Table 7. For selectivity between D4 and f2, the maximum frequency variation for the coordination range is 3.42 Hz. Thus, relay f2 can trip in 5s for $I^{2\emptyset}$. The frequency

TABLE 8. Operating times for a single-phase fault at bus 95.

Relay	Operating times (s)			
	Permanent fault		Temporary fault	
	P	N	P	N
R3	0.659	0.834	0.080	0.080
D3	0.154	0.553	0.060	0.060
D4	0.034	0.037	0.020	0.020
D5	0.068	0.074	0.020	0.020
f1	$\Delta f = 0.985Hz$ (Shall not trip)			
f2	$\Delta f = 1.051Hz$ (Shall not trip)			
f3	$\Delta f = 1.053Hz$ (Shall not trip)			

shift will be greater for a fault inside the microgrid, then f2 will trip in the instantaneous mode.

Fig. 8 shows the selectivity between D1 and V1 and between D4 and f2. For selectivity between D1 and V1, although the curves in the phase unit seem distant, the multiplication of the DG voltage in the pickup current makes the trip time between them very close, as shown in coordination times of Table 7. For selectivity between D4 and f2, the maximum frequency variation for the coordination range is 3.42 Hz. Thus, relay f2 can trip in 5s for $I^{2\emptyset}$. The frequency shift will be greater for a fault inside the microgrid, then f2 will trip in instantaneous mode.

A fault current $I_5^{1\emptyset}$ at bus 95 is considered to exemplify and evaluate the proposed solution. Table 8 shows the operating times for temporary and permanent faults. During a temporary fault, D3, D4, and D5 trip on the 50TD characteristic first than R3, allowing the recloser to de-energize the section and eliminate the fault. At the same time, frequency relays shall not trip to avoid miscoordination.

During a permanent fault, neutral units of D3, D4, and D5 trip, changing the microgrids' status to islanded operation before the recloser trip. Posteriorly, R3 in 51(P) characteristic trip and isolate the faulty zone, ensuring the safety of distribution network devices and minimizing the energy not supplied. Thus, during the repair time, customers upstream R3 and inside MG3, MG4, and MG5 remain energized, improving reliability indices. Therefore, the proposed solution allows the proper operation of microgrids in distribution networks.

IV. CONCLUSION

This paper proposes a mathematical model to solve the optimal coordination problem of protection devices in distribution networks with microgrids, including renewable distributed generation and energy storage systems.

The proposed methodology provides good results since the operating times of protection devices have values close to limits imposed by the constraints, despite the optimal solution not being guaranteed. Nevertheless, the quality and processing speed (143 seconds) are attractive, providing quick information for decision-making in planning projects. The achieved coordination and selectivity to all protection devices considered in the study case are feasible, providing low operating times. DOCRs and local protections ensure the safe operation of microgrids.

Microgrids usually include many protection devices, despite these protection devices being redundant. Both the PCC and the PoC have a single protection device in the proposed methodology. A future proposal should include redundant protection devices to reinforce the microgrid reliability in parallel and islanded operation modes.

The proposed methodology allows a proper operation of microgrids in the distribution system, maximizing the benefits provided by this technology. Moreover, microgrids improve the quality and continuity of the electricity supply service, encouraging the evolution of distribution systems due to their influence on the expansion planning and distribution network operation. The results obtained by the proposed methodology raise expectations about this scenario.

REFERENCES

[1] A. C. Moreira, H. K. M. Paredes, W. A. de Souza, F. P. Marafao, and L. C. P. da Silva, "Intelligent expert system for power quality improvement under distorted and unbalanced conditions in three-phase AC microgrids," *IEEE Trans. Smart Grid*, vol. 9, no. 6, pp. 6951–6960, Nov. 2018, doi: 10.1109/TSG.2017.2771146.

[2] M. K. Sharma, P. Kumar, and V. Kumar, "Intentional islanding of microgrid," in *Proc. 6th Int. Conf. Comput. Appl. Electr. Eng.-Recent Adv. (CERA)*, Oct. 2017, pp. 247–251, doi: 10.1109/CERA.2017.8343335.

[3] K. Pereira, B. R. Pereira, J. Contreras, and J. R. S. Mantovani, "A multiobjective optimization technique to develop protection systems of distribution networks with distributed generation," *IEEE Trans. Power Syst.*, vol. 33, no. 6, pp. 7064–7075, Nov. 2018, doi: 10.1109/TPWRS.2018.2842648.

[4] P. Alaee and T. Amraee, "Optimal coordination of directional overcurrent relays in meshed active distribution network using imperialistic competition algorithm," *J. Modern Power Syst. Clean Energy*, vol. 9, no. 2, pp. 416–422, 2021, doi: 10.35833/MPCE.2019.000184.

[5] S. Kamel, A. Korashy, A.-R. Youssef, and F. Jurado, "Development and application of an efficient optimizer for optimal coordination of directional overcurrent relays," *Neural Comput. Appl.*, vol. 32, no. 12, pp. 8561–8583, Jun. 2020, doi: 10.1007/s00521-019-04361-z.

[6] J. Yu, C.-H. Kim, and S.-B. Rhee, "The comparison of lately proposed Harris hawks optimization and Jaya optimization in solving directional overcurrent relays coordination problem," *Complexity*, vol. 2020, pp. 1–22, Jan. 2020, doi: 10.1155/2020/3807653.

[7] J. Shah, N. Khristi, V. N. Rajput, and K. S. Pandya, "A new objective function for optimal coordination of directional over-current relays," *Adv. Electr. Power Energy Infrastruct.*, vol. 608, pp. 1–11, Jan. 2020, doi: 10.1007/978-981-15-0206-4_1.

[8] D. Vyas, P. Bhatt, and V. Shukla, "Coordination of directional overcurrent relays for distribution system using particle swarm optimization," *Int. J. Smart Grid Clean Energy*, vol. 9, no. 2, pp. 290–297, 2020, doi: 10.12720/sgce.9.2.290-297.

[9] A. A. Kida, A. E. L. Rivas, and L. A. Gallego, "An improved simulated annealing–linear programming hybrid algorithm applied to the optimal coordination of directional overcurrent relays," *Electric Power Syst. Res.*, vol. 181, Apr. 2020, Art. no. 106197, doi: 10.1016/j.epsr.2020.106197.

[10] A. M. Entekhabi-Nooshabadi, H. Hashemi-Dezaki, and S. A. Taher, "Optimal microgrid's protection coordination considering N-1 contingency and optimum relay characteristics," *Appl. Soft Comput.*, vol. 98, Jan. 2021, Art. no. 106741, doi: 10.1016/j.asoc.2020.106741.

[11] K. A. Saleh, H. H. Zeineldin, and E. F. El-Saadany, "Optimal protection coordination for microgrids considering N-1 contingency," *IEEE Trans. Ind. Informat.*, vol. 13, no. 5, pp. 2270–2278, Oct. 2017, doi: 10.1109/TII.2017.2682101.

[12] M. Usama, M. Moghavvemi, H. Mokhlis, N. N. Mansor, H. Farooq, and A. Pourdaryaei, "Optimal protection coordination scheme for radial distribution network considering ON/OFF-grid," *IEEE Access*, vol. 9, pp. 34921–34937, 2021, doi: 10.1109/ACCESS.2020.3048940.

[13] S. D. Saldarriaga-Zuluaga, J. M. López-Lezama, and N. Muñoz-Galeano, "Optimal coordination of over-current relays in microgrids considering multiple characteristic curves," *Alexandria Eng. J.*, vol. 60, no. 2, pp. 2093–2113, Apr. 2021, doi: 10.1016/j.aej.2020.12.012.

[14] S. D. Saldarriaga-Zuluaga, J. M. López-Lezama, and N. Muñoz-Galeano, "An approach for optimal coordination of over-current relays in microgrids with distributed generation," *Electronics*, vol. 9, no. 10, pp. 1–15, 2020, doi: 10.3390/electronics9101740.
[15] R. Tiwari, R. K. Singh, and N. K. Choudhary, "Optimal coordination of dual setting directional over current relays in microgrid with different standard relay characteristics," in *Proc. IEEE 9th Power India Int. Conf. (PIICON)*, Feb. 2020, pp. 1–6, doi: 10.1109/PIICON49524.2020.9112883.
[16] H. Beder, B. Mohandes, M. S. E. Moursi, E. A. Badran, and M. M. E. Saadawi, "A new communication-free dual setting protection coordination of microgrid," *IEEE Trans. Power Del.*, vol. 36, no. 4, pp. 2446–2458, Aug. 2021, doi: 10.1109/TPWRD.2020.3041753.
[17] K. Sarwagya, P. K. Nayak, and S. Ranjan, "Optimal coordination of directional overcurrent relays in complex distribution networks using sine cosine algorithm," *Electr. Power Syst. Res.*, vol. 187, Oct. 2020, Art. no. 106435, doi: 10.1016/j.epsr.2020.106435.
[18] *Measuring Relays and Protection Equipment—Part 151: Functional Requirements for Over/Under Current Protection*, Standard 60255-151, Dublin, Republic of Ireland, 2009.
[19] M. N. Alam, B. Das, and V. Pant, "Protection coordination scheme for directional overcurrent relays considering change in network topology and OLTC tap position," *Electr. Power Syst. Res.*, vol. 185, Aug. 2020, Art. no. 106395, doi: 10.1016/j.epsr.2020.106395.
[20] C. A. Plet, M. Graovac, T. C. Green, and R. Iravani, "Fault response of grid-connected inverter dominated networks," in *Proc. IEEE PES Gen. Meeting*, Jul. 2010, pp. 1–8, doi: 10.1109/PES.2010.5589981.
[21] R. F. Buzo, H. M. Barradas, and F. B. Leão, "Fault current of PV inverters under grid-connected operation: A review," *J. Control, Autom. Electr. Syst.*, vol. 32, no. 4, pp. 1053–1062, Aug. 2021, doi: 10.1007/s40313-021-00729-6.
[22] S&C ELECTRIC COMPANY. (2020). *Positrol Fuse Links*. Accessed: Aug. 11, 2021. [Online]. Available: http://www.sandc.com/en/products–%0Aservices/products/positrol-fuse-links/
[23] *Standard for Interconnection and Interoperability of Distributed Energy Resources With Associated Electric Power Systems Interfaces*, Standard 1547, New York, NY, USA, 2018.
[24] J. C. M. Vieira, W. Freitas, W. Xu, and A. Morelato, "Efficient coordination of ROCOF and frequency relays for distributed generation protection by using the application region," *IEEE Trans. Power Del.*, vol. 21, no. 4, pp. 1878–1884, Oct. 2006, doi: 10.1109/TPWRD.2006.881588.
[25] H. Bevrani, A. Ghosh, and G. Ledwich, "Renewable energy sources and frequency regulation: Survey and new perspectives," *IET Renew. Power Gener.*, vol. 4, no. 5, pp. 438–457, Sep. 2010, doi: 10.1049/iet-rpg.2009.0049.
[26] M. H. Marcolino, J. B. Leite, and J. R. Sanches Mantovani, "Optimal coordination of overcurrent directional and distance relays in meshed networks using genetic algorithm," *IEEE Latin Amer. Trans.*, vol. 13, no. 9, pp. 2975–2982, Sep. 2015, doi: 10.1109/TLA.2015.7350048.
[27] L. G. W. da Silva, R. A. F. Pereira, and J. R. S. Mantovani, "Allocation of protective devices in distribution circuits using nonlinear programming models and genetic algorithms," *Electr. Power Syst. Res.*, vol. 69, no. 1, pp. 77–84, 2003, doi: 10.1016/j.epsr.2003.08.010.
[28] L. G. W. D. Silva, R. A. F. Pereira, and J. R. S. Mantovani, "Alocação otimizada de dispositivos de controle e proteção em redes de distribuição," *Sba, Controle Automação Sociedade Brasileira de Automatica*, vol. 21, no. 3, pp. 294–307, Jun. 2010, doi: 10.1590/s0103-17592010000300007.
[29] LAPSEE. (2018). *Distribution System Testing—135 Buses*. Accessed: Jun. 11, 2021. [Online]. Available: https://www.feis.unesp.br/#!/departamentos/engenharia-eletrica/pesquisas-e-projetos/lapsee/downloads/materiais-de-cursos1193/

CLEBERTON REIZ (Graduate Student Member, IEEE) received the B.Sc. degree in electrical engineering from Mato Grosso State University (UNEMAT), Sinop, Brazil, in 2017, and the M.Sc. degree in electrical engineering from São Paulo State University (UNESP), Ilha Solteira, Brazil, in 2019, where he is currently pursuing the Ph.D. degree. Since 2021, he has been a Visiting Student with the Institute for Systems and Computer Engineering, Technology and Science (INESC TEC), Porto, Portugal. His current research interests include the development of methods for the optimization, planning, and control of electrical power systems.

JONATAS BOAS LEITE (Member, IEEE) received the B.Sc. and Ph.D. degrees in electrical engineering from São Paulo State University (UNESP), Ilha Solteira, Brazil, in 2010 and 2015, respectively. He was a Postdoctoral Researcher with the Electrical and Computer Engineering Department, Texas A&M University, College Station, TX, USA, and the Electrical Engineering Postgraduate Program of UNESP, in 2016 and 2019, respectively, where he is currently a Professor with the Department of Electrical Engineering and the Laboratorio de Planejamento de Sistemas de Energia Eletrica, Ilha Solteira. His research interests include planning and control of electrical power systems.